THE ASTROPHYSICAL JOURNAL, 438:269–287, 1995 January 1

CHROMOSPHERIC VARIATIONS IN MAIN-SEQUENCE STARS. II.[1]

S. L. BALIUNAS,[2,3,4] R. A. DONAHUE,[2] W. H. SOON,[2] J. H. HORNE,[5] J. FRAZER,[6] L. WOODARD-EKLUND,[7,8]
M. BRADFORD,[6] L. M. RAO,[9,13] O. C. WILSON,[6,10] Q. ZHANG,[2] W. BENNETT,[6] J. BRIGGS,[8,11]
S. M. CARROLL,[12,13] D. K. DUNCAN,[14] D. FIGUEROA,[6] H. H. LANNING,[8,15] A. MISCH,[8,16]
J. MUELLER,[8,17] R. W. NOYES,[2] D. POPPE,[6] A. C. PORTER,[10,13,18] C. R. ROBINSON[13,19]
J. RUSSELL,[6] J. C. SHELTON,[6] T. SOYUMER,[6]
A. H. VAUGHAN,[8,20] AND J. H. WHITNEY[13,21]

Received 1994 May 5; accepted 1994 July 5

ABSTRACT

The fluxes in passbands 0.1 nm wide and centered on the Ca II H and K emission cores have been monitored in 111 stars of spectral type F2–M2 on or near the main sequence in a continuation of an observing program started by O. C. Wilson. Most of the measurements began in 1966, with observations scheduled monthly until 1980, when observations were scheduled several times per week. The records, with a long-term precision of about 1.5%, display fluctuations that can be identified with variations on timescales similar to the 11 yr cycle of solar activity as well as axial rotation, and the growth and decay of emitting regions. We present the records of chromospheric emission and general conclusions about variations in surface magnetic activity on timescales greater than 1 yr but less than a few decades.

The results for stars of spectral type G0–K5 V indicate a pattern of change in rotation and chromospheric activity on an evolutionary timescale, in which (1) young stars exhibit high average levels of activity, rapid rotation rates, no Maunder minimum phase and rarely display a smooth, cyclic variation; (2) stars of intermediate age ($\sim$1–2 Gyr for 1 $M_\odot$) have moderate levels of activity and rotation rates, and occasional smooth cycles; and (3) stars as old as the Sun and older have slower rotation rates, lower activity levels, and smooth cycles with occasional Maunder minimum-phases.

Subject headings: stars: activity — stars: chromospheres — stars: late-type — stars: rotation

> I am at last convinced that the spots are objects close to the surface of the solar globe ... also that they are carried round the Sun by its rotation ... .—GALILEO, *Historia e Dimostrazioni intorno alle Macchie Solari* (1613).

1. INTRODUCTION

Telescopic observations of sunspots, begun by Galileo, Scheiner, and other early solar physicists, comprise a record showing increases and decreases in sunspots roughly every 11 yr (Schwabe 1843; Wolf 1856). Because sunspots are magnetic in nature (Hale 1908), the 11 yr cycle is a variation in surface magnetism.[22] Other surface inhomogeneities measured in modern times (see Rosner, Golub, & Vaiana 1985) also link magnetism to the cycle. Geologic records such as ^{14}C and ^{10}Be (Damon 1977; Damon & Sonnett 1991; Beer et al. 1990) extend information on solar magnetic variations to the last several millenia. Taken together, the sunspot and geologic records indicate variability on timescales longer than 11 yr: roughly every few centuries solar magnetism drops to levels lower than that of the minima between cycles, e.g., the Maunder Minimum (circa 1645–1720; Spörer 1887, 1889; Maunder 1890, 1894; Eddy 1976). However, despite records spanning several millenia, the explanation of solar magnetic activity and its variations remains recondite.

The observations of variations in magnetic activity on the Sun have stimulated theoretical explanations such as a hydromagnetic dynamo or an internal torsional oscillator. In

[1] This paper is dedicated to Olin Wilson.

[2] Harvard-Smithsonian Center for Astrophysics, 60 Garden Street, Cambridge, MA 02138.
[3] Also Center of Excellence in Information Systems at Tennessee State University, 330 10th Avenue North, Nashville, TN 37203.
[4] Robert Wesson Fellow, Hoover Institution, Stanford CA, 94305.
[5] Department of Physics, Yale University, 217 Prospect Street, New Haven, CT 06520.
[6] Mount Wilson Observatory, Mount Wilson, CA 91023.
[7] Department of Astronomy, University of California at Los Angeles, 405 Hilgard Avenue, Los Angeles, CA 90024.
[8] Also Mount Wilson Observatory.
[9] Department of Astronomy, University of Wisconsin, 475 North Charter Street, Madison, WI 53706.
[10] Deceased.
[11] Yerkes Observatory, 373 West Geneva Street, Williams Bay, WI 53191.
[12] Center for Theoretical Physics, Laboratory for Nuclear Science and Department of Physics, Massachusetts Institute of Technology, Cambridge, MA 02139.
[13] Also Harvard-Smithsonian Center for Astrophysics.
[14] Department of Astronomy and Astrophysics, University of Chicago; and Adler Planetarium, 5640 South Ellis Avenue, Chicago, IL 60637.
[15] Computer Sciences Corporation, Space Telescope Science Institute, 3700 San Martin Drive, Baltimore, MD 21218.
[16] Lick Observatory, Santa Cruz, CA 95064.
[17] Palomar Observatory, Palomar Mountain, CA 92060.
[18] NOAO, P.O. Box 26732, Tucson, AZ 85726.
[19] Department of Astronomy and Astrophysics, The Pennsylvania State University, 525 Davey Laboratory, University Park, PA 16802.
[20] Jet Propulsion Laboratory, Office of Space Science and Instrumentation, 4800 Oak Grove Drive, Pasadena, CA 91109.
[21] Department of Astronomy, University of Virginia, P.O. Box 3818, University Station, Charlottesville, VA 22903.

[22] The Sun also exhibits a magnetic polarity reversal in sunspot pairs between the northern and southern hemispheres that produces the 22 yr period of magnetic activity (Hale & Nicholson 1925). The polarity and its phase are not measured for other stars in this experiment and are therefore not discussed.

dynamo theory, the internal motions of differential rotation and convection maintain the magnetic fields responsible for the sunspot cycle (Parker 1955; Steenbeck, Krause, & Rädler 1966; Rosner & Weiss 1992). In the torsional oscillator theory, the observed oscillations of surface magnetic field originate from an interaction between a nonregenerative primordial field and internal differential rotation in the radiative core (see Gough 1990). Both explanations have had limited success thus far, largely because of the lack of knowledge about the physical conditions of the solar interior, as well as the complexity of the calculations. Progress may come from advances in information about the interior motions of the Sun, for example, by resolving more completely the frequencies of *p*-mode splitting in the 5 minute oscillations (Brown & Morrow 1987; Gough & Toomre 1991).

Areas of concentrated magnetic field on the Sun emit Ca II H (396.8 nm) and K (393.4 nm) more intensely than areas with less magnetic field present. The intensity of H and K emission increases in response to the amount of nonthermal heating of the chromosphere, e.g., heating produced by local magnetic inhomogeneities, and is a useful spectroscopic indicator of the strength of, and area covered by, magnetic fields (Leighton 1959). Ca II emission intensity corresponds on roughly a one-to-one basis with the product of the magnetic field strength and area coverage (Skumanich, Smythe, & Frazier 1975; Schrijver et al. 1989). Thus, records of disk-integrated Ca II measurements of the Sun trace changes in surface activity caused by, for example, the activity cycle or stellar rotation (Hale & Fox 1908; Bumba & Růžičková-Topolová 1967; Sheeley 1967; White & Livingston 1978, 1981; Keil & Worden 1984).

Ca II H and K emission has been studied systematically in lower main-sequence stars for nearly four decades beginning with Wilson & Bappu (1957). Several properties of chromospheric activity have been derived from cross-sectional studies of the instantaneous or time-averaged flux of H and K emission in main-sequence stars.

First, Ca II H and K emission is observed in stars later than approximately F0–F2 V, i.e., less massive than about 1.5 $M_{\odot}$, although the range of masses that can support solar-like magnetic activity is imprecisely known (Wolff, Boesgaard, & Simon 1986; Schrijver & Rutten 1987; Mullen & Cheung 1993; Schrijver 1993). The appearance of H and K emission roughly coincides with the establishment of nonnegligible subsurface convection along the lower main sequence (Hoyle & Wilson 1958), and the intensity of H and K emission weakens with age on the main sequence (Wilson 1963). The onset of substantial convective zones and H and K emission also coincides with a corresponding decline in the average angular momentum per unit mass along the main sequence which decreases with advancing age (Wilson 1966; Kraft 1967). On the Sun and, presumably, lower main-sequence stars, the magnetic field not only heats but also permeates the outer atmospheric layers and carries away angular momentum in a magnetized wind (Schatzman 1962; Parker 1965). Over eons on the main sequence, that loss of angular momentum appreciably slows the rotation of a star and causes the average magnetic activity level to subside because rotation aids in driving the production of surface magnetic activity.

Moreover, information on the initial values and early history of a star's magnetic field and angular momentum is quickly lost once the star reaches the main sequence (e.g., Stauffer 1991). That is, the process that generates magnetic fields in lower main-sequence stars eradicates evidence of prior conditions. That process produces nearly uniform levels of average chromospheric emission and rotation among stars of similar mass (i.e., the depth of the convective zone) and age.

The ubiquity of H and K emission (Schwarzschild & Eberhard 1913) suggests that surface magnetic activity is a universal phenomenon in lower main-sequence stars. The previously mentioned cross-sectional studies of surface activity can be complemented by time-serial studies that seek to illuminate both the existence of average levels of activity and their time dependence. Comparing the variability of H and K emission in main-sequence stars should provide important validation for theories of magnetic activity, as well as place solar activity in a general perspective.

Observations of chromospheric variability require at least a decade to reveal variations with timescales similar to the 11 yr solar cycle. Such a program was initiated by Wilson (1968, 1978), who discovered the widespread occurrence of activity cycles by monitoring H and K variations in 91 stars on or near the lower main sequence over 12 yr. We have extended Wilson's initial records to 25 yr and added new stars to bring the total in the monitoring program to 111 stars.

2. OBSERVATIONS

Two sets of measurements have been combined to make 25 yr records of stellar chromospheric activity. Wilson (1978) made observations from 1966 to 1977 at monthly intervals on the 100 inch (2.5 m) telescope at Mount Wilson Observatory. The survey moved in 1977 to the 60 inch (1.5 m) telescope with an instrument whose measurements can be compared to those of Wilson's system (Vaughan, Preston, & Wilson 1978). The purpose of the move was to increase the size of the sample and frequency of observations. Near-nightly measurements starting in 1980 reveal rotation (Vaughan et al. 1981; Baliunas et al. 1983) that is suggested but temporally unresolved in the earlier data (Wilson 1978). Observations are included through 1991 March 31. The number of individual observations presented here is 171,300.

2.1. *Wilson's Program, 1966–1977*

Wilson (1968) began measurements of the 91 stars in his published program in 1966 March with the 100 inch telescope and coudé scanner with a two-channel photometer. The device recorded the fluxes in either the H or the K channel relative to the combined monitor channels. The width of the scanning slit is 0.1 nm, which was tuned to compensate for the Doppler velocity of Earth relative to each star. The two fixed monitor channels are 2.5 nm wide and situated in the continuum on either side of the H–K region and separated by about 25 nm. The counts in each channel were corrected for sky and instrumental background illumination.

The ratio of the counts in the H and K lines relative to those of the monitor channels was adjusted nightly to correct for instrumental variations. The correction factor was determined from measurements of a standard lamp. That combined relative flux, defined by Wilson as F, is an average of the separate, corrected measures of the H and K fluxes relative to the monitor channels.

2.2. *Continued Monitoring, 1977–Present*

The system originally designed for the 60 inch telescope has been operating since 1977 and is fully described by Vaughan et al. (1978). Briefly, it consists of a grating spectrometer, a single

photomultiplier, and rotating mask with four slots spinning at a rate of about 30 Hz. The 30 Hz sampling rate allows one photomultiplier tube to record all four channels independently but rapidly enough to be considered as simultaneous with respect to atmospheric fluctuations. Two narrow (0.1 nm) passbands measure the chromospheric H and K fluxes, and two 2.0 nm passbands sample the photospheric fluxes at 390.1 nm and 400.1 nm.

The system has been upgraded several times and now includes a slit mask (changed in 1982) that allows the choice of a 0.1 nm or 0.2 nm wide slit for the H and K lines, and a chopper wheel (changed in 1983; Duncan et al. 1984) that samples H and K fluxes simultaneously for increased throughput. The mask containing the exit slits are translated to correct for Doppler shifts which are computed nightly for each star's relative velocity. A hollow cathode lamp produces an emission spectrum whose narrow H and K lines are used to calibrate the origin of the radial velocity scale several times per night.

The observed quantity, S, is defined as

$$S = \alpha \frac{H + K}{V + R}, \quad (1)$$

where H and K are the counts in the combined Ca II passbands, and V and R are the counts in the violet and red continuum bands, corrected for sky and instrument background. S is assumed to be a general indicator of chromospheric activity related to the strength and area of magnetic activity on a star (Schrijver et al. 1989). The quantity, α, is a calibration factor that changes nightly and is determined from the standard lamp and the measurements of the standard stars. Between 1977 and the middle of 1980, observations of standard stars provide the value of α. After 1980, the standard lamp and standard stars are used to reckon the value of α. A detailed paper describing this process is in preparation.

The widths of the H and K emission cores increase with increasing luminosity (Wilson & Bappu 1957) so that evolved stars have emission cores slightly wider than the 0.1 nm slit widths. A few evolved stars in the survey (HD 3795, HD 23249, HD 88737, HD 124850, and HD 188512) were measured starting in 1983 with the 0.2 nm passband for about a year. In order to maintain continuity, we reverted to monitoring these few stars with the narrower slit. The few data obtained with the 0.2 nm slit have been transformed to the scale of the 0.1 nm by measurements from each slit made nearly simultaneously.

2.3. *Estimate of Long-Term Precision*

Wilson monitored 18 standard stars. We eliminated the use of the star HD 161239 (84 Her) as a standard because Wilson noted that the star displayed notable long-term fluctuations (see Appendix A). The 17 stars we used as standards are listed in Table 1 in order of increasing Henry Draper (HD) number along with $B-V$, and the percent standard deviation of S computed over the 25 yr record. The average of S over the record is computed from means in 30 day intervals in order to avoid skewing the means by the intensively sampled data taken after 1980. The 17 standard stars are distributed across the sky, so that on any night several standard stars are accessible. On average, four standard stars are observed on a given night.

The observed flux in the faintest channel (usually the K passband) dictates the integration time required to reduce the uncertainty caused by photon statistics to 1.0%–1.5%. Measurements at the 60 inch telescope employed integration times intended to yield this precision. Occasionally, weather conditions meant sacrificing counting precision for surveying the entire list of accessible stars on a given night.

TABLE 1

STANDARD STARS

HD Number	$B-V$	$\langle\sigma_S/S\rangle$
9562	0.64	1.4%
13421	0.56	1.4
29645	0.57	1.4
45067	0.56	1.1
76572[a]	0.43	2.0
89744	0.54	1.2
107213	0.50	1.5
124570	0.54	0.9
136202[a]	0.54	2.2
142373	0.56	0.8
143761	0.60	1.0
159332	0.48	1.6
187013[a]	0.47	2.2
187691[a]	0.55	1.5
207978	0.42	1.0
212754	0.52	1.3
216385	0.48	0.8
Mean $\langle\sigma_S/S\rangle$ (17 stars)		1.4%
Mean $\langle\sigma_S/S\rangle$ (13 stars)		1.2%

NOTE.—The mean $\langle\sigma_S/S\rangle$ should represent the upper limit of long-term precision. The least variable stars in this table have $\langle\sigma_S/S\rangle \approx 0.8\%$–$1.0\%$. Not all stars with low variability are standards. As observations progressed, stars not initially chosen as standards were revealed to be nearly nonvariable (e.g., HD 10700 with $\langle\sigma_S/S\rangle \approx 1.2\%$).

[a] The star may not be suitable as a standard star because some long-term variability is evident in the record (see Fig. 1, Table 2), and, in general, $\langle\sigma_S/S\rangle \gtrsim 1.5\%$.

The primary calibration standard is the lamp whose measurements have higher counts and more statistical precision than the standard stars, which may vary with amplitudes comparable to the system's threshold for detecting variability. We computed a night-to-night precision of $\sim 0.5\%$ (s.d.) from the mean for the measurements of the lamp. The lamp reveals systematic instrumental variations that can occur from night to night and are also evident in the observations of the standard stars. However, the lamp occasionally exhibits changes which are not present in the measurements of the standard stars, i.e., changes that are caused by variations in the lamp itself. In that case, we substituted the calibration factor provided by the less precise measurements of the standard stars. The combined approach of a lamp, confirmed by the standard stars, or, occasionally, those stars alone, yields a long-term (25 yr) precision of stellar records of $\sim 1.4\%$ s.d., based on the average standard deviation of the 17 standard stars. After the calibration, four standard stars appear to have low amplitude but significant variations (Table 1). Eliminating those four stars yields a slightly improved estimate of long-term precision, 1.2%.

2.4. *Solar Chromospheric Data*

The record of solar chromospheric variations is an important point of comparison to stellar activity records. In that connection, Wilson (1978) made observations of the Moon as a

proxy of the disk-integrated sunlight with the two-channel photometer of the 100 inch telescope at roughly monthly intervals in 1966–1971 and 1974–1977. In 1980 the afternoon sky was monitored with the instrument on the 60 inch telescope in order to discern the *timescale*, but not the amplitude, of variations (Baliunas et al. 1983). Rayleigh scattering in the Earth's atmosphere reduces the contrast of the observed solar H and K emission cores relative to the photospheric reference bands, which creates a systematic error in the value and amplitude of S in the record. Hence, the 1980 sky measurements have been omitted from the analysis of the solar records.

The solar record from 1975 onward is combined from two independent measurements of the disk-averaged Ca II K fluxes measured on the Sun. Observations have been made at Kitt Peak National Observatory (KPNO) by White & Livingston (1978, 1981) since late 1975, and at Sacramento Peak Observatory (SPO) since early 1977 (Keil & Worden 1984; Keil 1992).

White et al. (1992) compute a transformation of the KPNO measurements to Wilson's. However, the transformed KPNO data appear to be discrepant with the lunar observations in two respects. First, the transformed KPNO minima in 1976–1977 and 1985–1986 are approximately 5% higher than Wilson's. Second, the maximum of Cycle 20 (observed by Wilson) is approximately equal to the maxima of Cycles 21 and 22 transformed to the Wilson scale. However, Cycle 20 is much less active than Cycles 21 and 22 according to the 10.7 cm fluxes and sunspot numbers. The transformed SPO record also has similar problems, as seen in the distributions in Figure 2 of White et al. (1992). For example, the minima of neither solar record transformed by the calibration of White et al. drops to the observed minimum of the Wilson record.

We have independently converted the KPNO and SPO K-line fluxes to the S index. Our transformation differs from that of White et al. (1992) in one respect because we used the entire Wilson record instead of the averaged values at four phases of Cycle 20 listed in Table 1 of Wilson (1978). The Mount Wilson measurements have little overlap with the KPNO and SPO time series, which is a source of systematic error in transforming the solar measurements to the scale of the stellar measurements. Therefore, we used the 30 yr solar 10.7 cm record as an intermediary. We converted all three chromospheric time series (Wilson, KPNO, SPO) to the 10.7 cm record, and then transformed the combined time series back to S. The combined, transformed solar data are shown in Figure 1*d*. The transition between solar and lunar data at the 1976–1977 minimum is now smooth and the relative amplitudes of Cycles 20, 21, and 22 reflect those of the 10.7 cm and sunspot records. We believe our transformation of the solar records is consistent with Wilson's lunar observations and the solar proxies. We assume that those lunar measurements accurately link the solar and stellar data. The observed mean solar activity observed is $\langle S_\odot \rangle = 0.179$, slightly higher than the value given by Wilson (1978), owing to the inclusion of the more active Cycles 21 and 22. We began reobserving the Moon in 1993 in order to provide better coverage between our and other solar records.

2.5. *The Combined Time Series, 1966–Present*

The records for 111 stars on or near the lower main sequence and the Sun are shown in Figure 1. Wilson's data (*crosses*) were obtained over a few nights at monthly intervals on the 100 inch telescope between 1966 and 1977. Between 1977 and 1980, measurements (*triangles*) were made less frequently with the 60 inch telescope. Beginning in 1980, all points are plotted (*small dots*) with 30 day means (*open circles*) superposed. In the case of the Sun, crosses are Wilson's measurements of the full Moon (before 1978). Later data are the disk-integrated solar chromospheric measurements (*small dots*) transformed to the S index, superposed with monthly means (*open circles*), as discussed in the previous section. The monthly averages tend to reduce the rotational scatter.

The stars selected by Wilson (1968) range in spectral type from early F to early M and display a range of chromospheric emission. Wilson also chose some stars that are members of visual binary systems (see § 4.3). The visual binaries generally have orbital separations sufficiently large (greater than a few seconds of arc) so that the companions are resolved. In addition, the small orbital radial velocities produce little observed S-variation in the measured chromospheric flux. Known spectroscopic binaries with large amplitude orbital velocities were intended to be excluded (although see Appendix B for notes on possible or recently discovered binaries in the sample).

The sample is not complete in magnitude or distance. It includes only one M-type star, HD 95735 (Lalande 21185; M2.1 Ve). The sample of 111 stars contains Wilson's previously published 91 lower main-sequence stars, plus seven stars that he occasionally observed but did not report (HD 22072, HD 115617, HD 158614, HD 176051, HD 182572, HD 188512, and HD 190360), and 13 other stars added since 1977. The stars added most recently were of specific interest, e.g., HD 61421 (Procyon) and HD 129333 (see Appendix A). All data except Wilson's (pre-1977) observations of the aforementioned seven stars, whose records could not be accurately transformed to S-values, are plotted.

The activity records in Figure 1 are grouped by $B-V$ with the pages in order of increasing $B-V$; since most of the stars in the sample are dwarfs, the pages are roughly in order of decreasing main-sequence mass. Within each mass grouping, stars with high $\langle S \rangle$-values are near the top and low $\langle S \rangle$-values near the bottom of the page. The HD number, $B-V$ color index, and summary of long-term variability are listed at the top of each star's panel. Table 2 lists the results for the Sun and the stars in order of increasing HD number and also includes a cross-reference to Figure 1.

3. ANALYSIS

We classify the long-term variations primarily on the basis of results from calculations of power spectra of the time series. The classification has an important bias—namely, it assumes that long-term variations should be cyclic, similar to the solar activity cycle. As we shall see, classifications other than cyclic exist, i.e., *var* (significant variability with no clear period from the power spectrum analysis), *flat* (no significant variability), *flat*? (possible low-amplitude variability) and *long* (variability on timescales longer than about 20 yr). These terms are defined in the notes to Table 2.

We computed periodograms (Scargle 1982) for each stellar record in order to search for activity cycles, P_{cyc} (variations $\gg 1$ yr). A periodogram calculated by this method has several useful properties. First, unevenly sampled data are treated in an unbiased way. Second, the significance of the height of the tallest peak of the periodogram can be estimated by the false alarm probability, FAP (Scargle 1982; Horne & Baliunas 1986). The FAP (expressed in percent) is the likelihood that a peak of height z or higher would occur *assuming the data are*

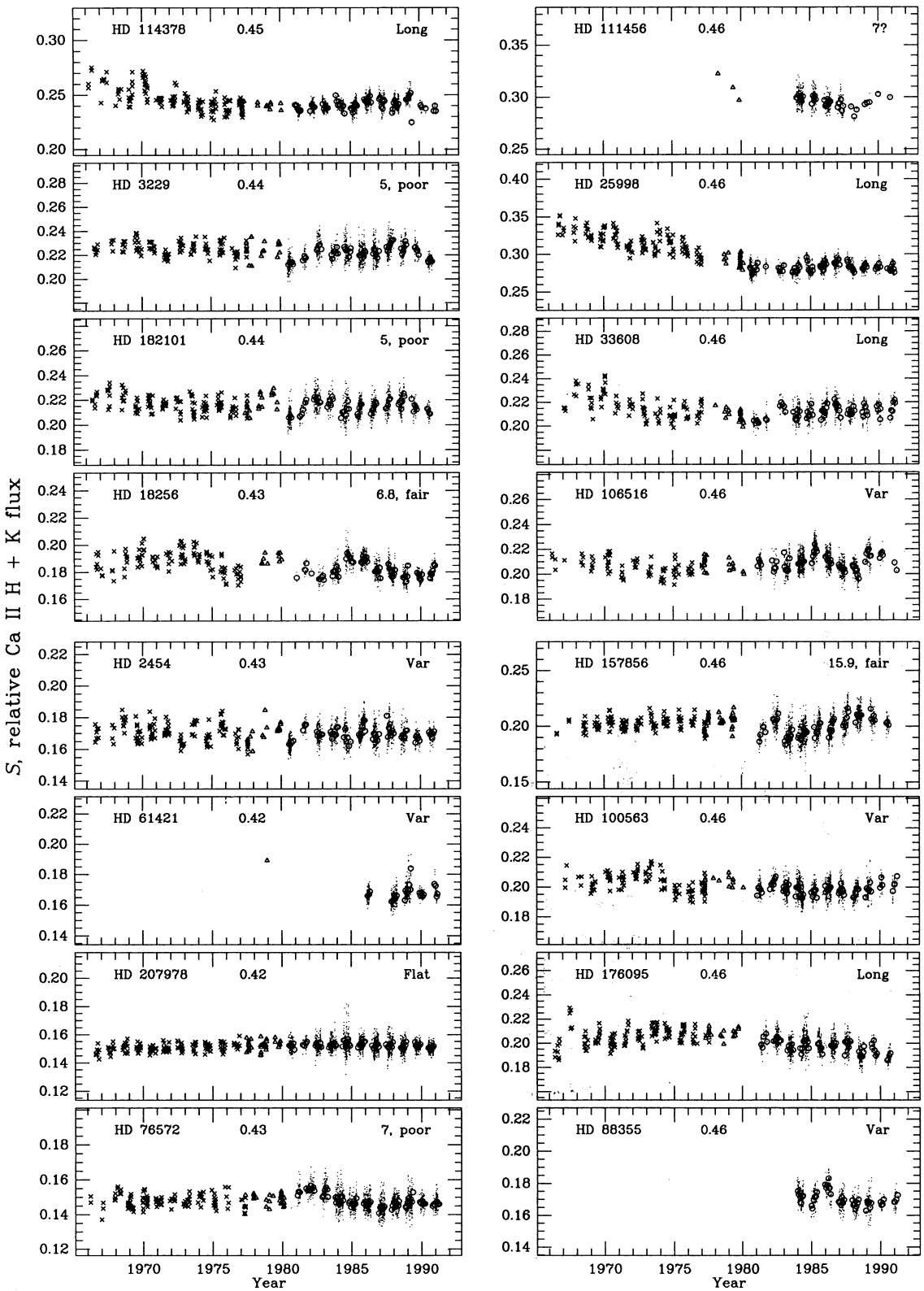

FIG. 1*a*

FIG. 1.—Records of relative Ca II emission fluxes, in units of *S*

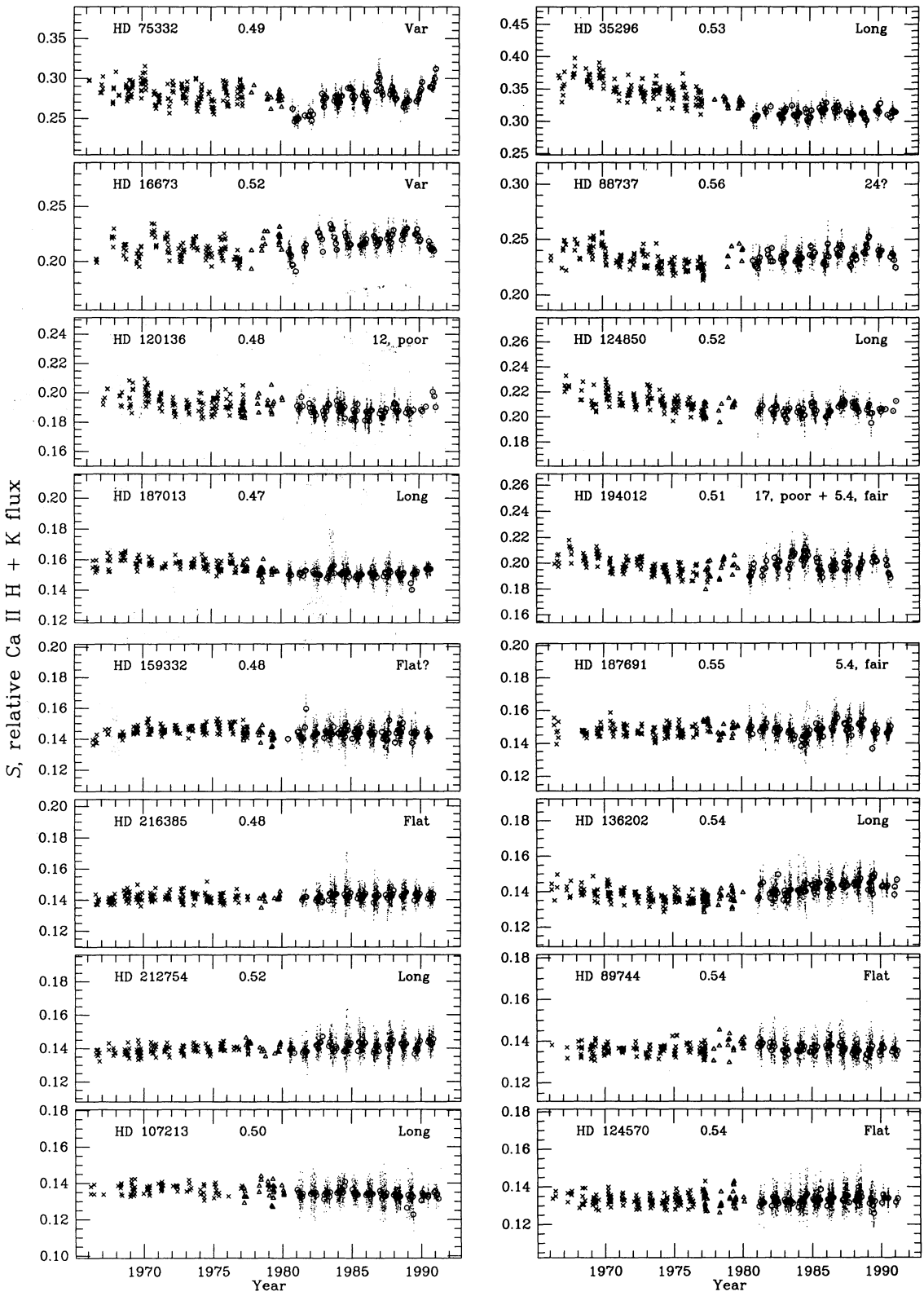

FIG. 1*b*

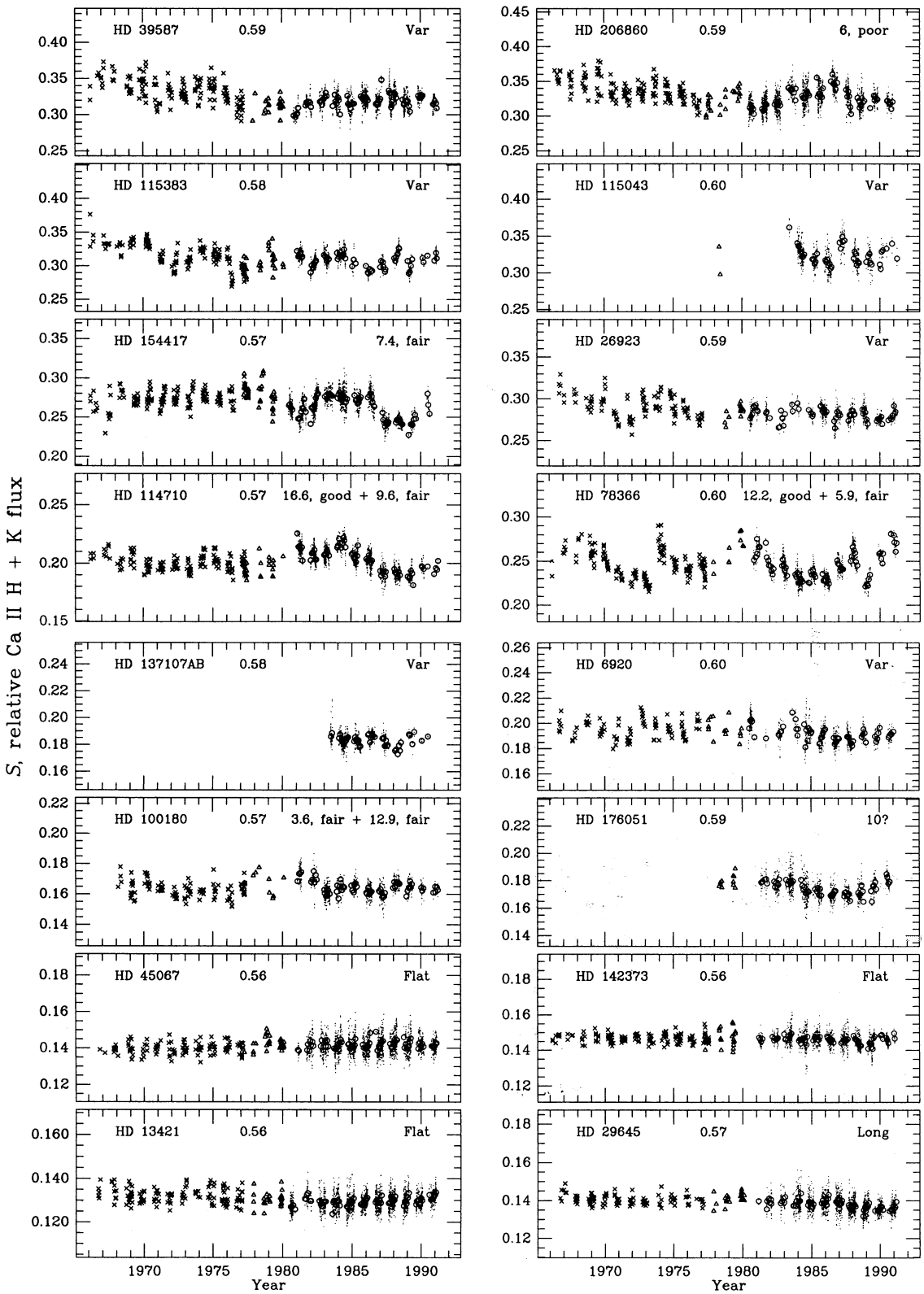

FIG. 1*c*

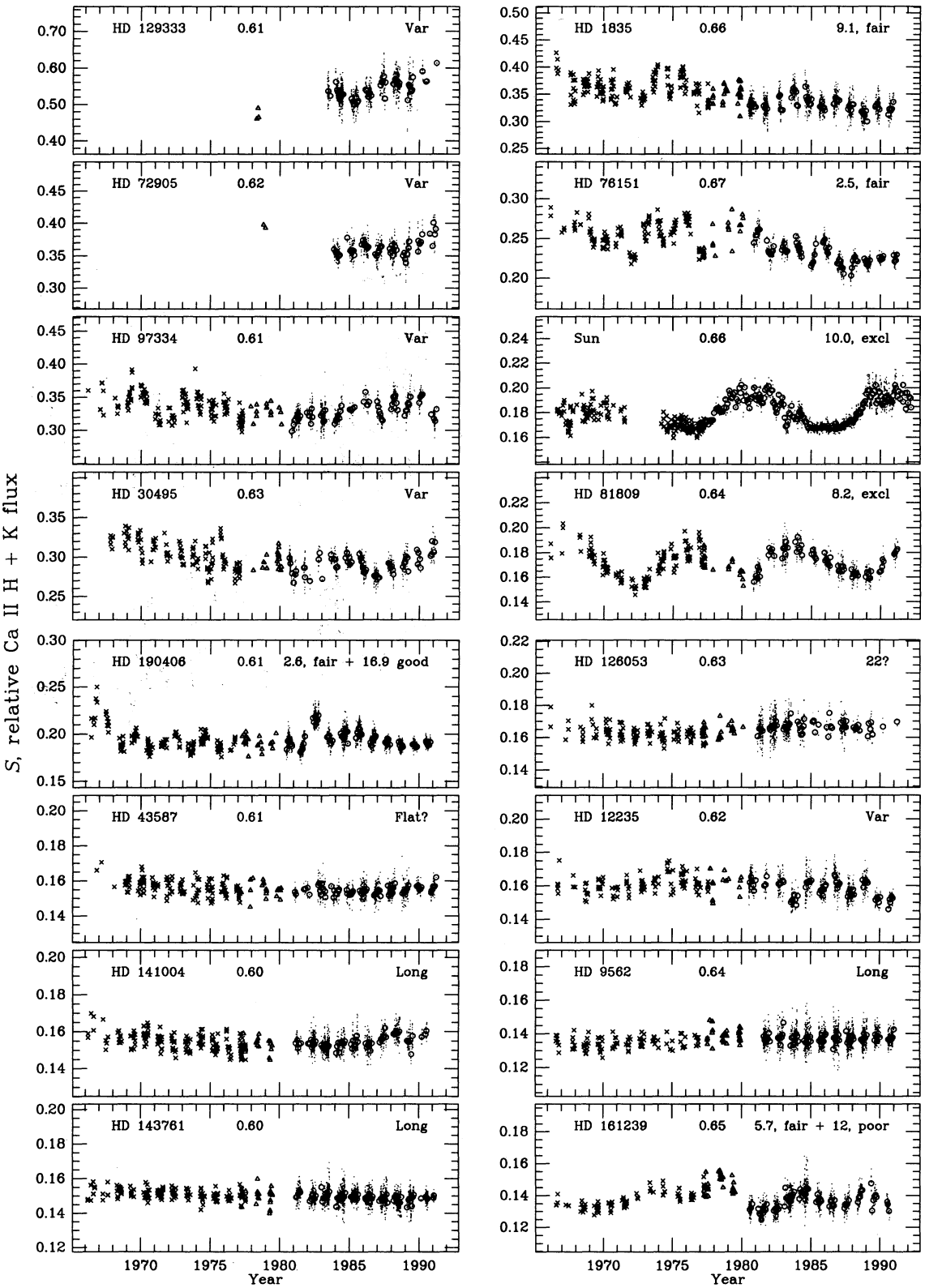

FIG. 1*d*

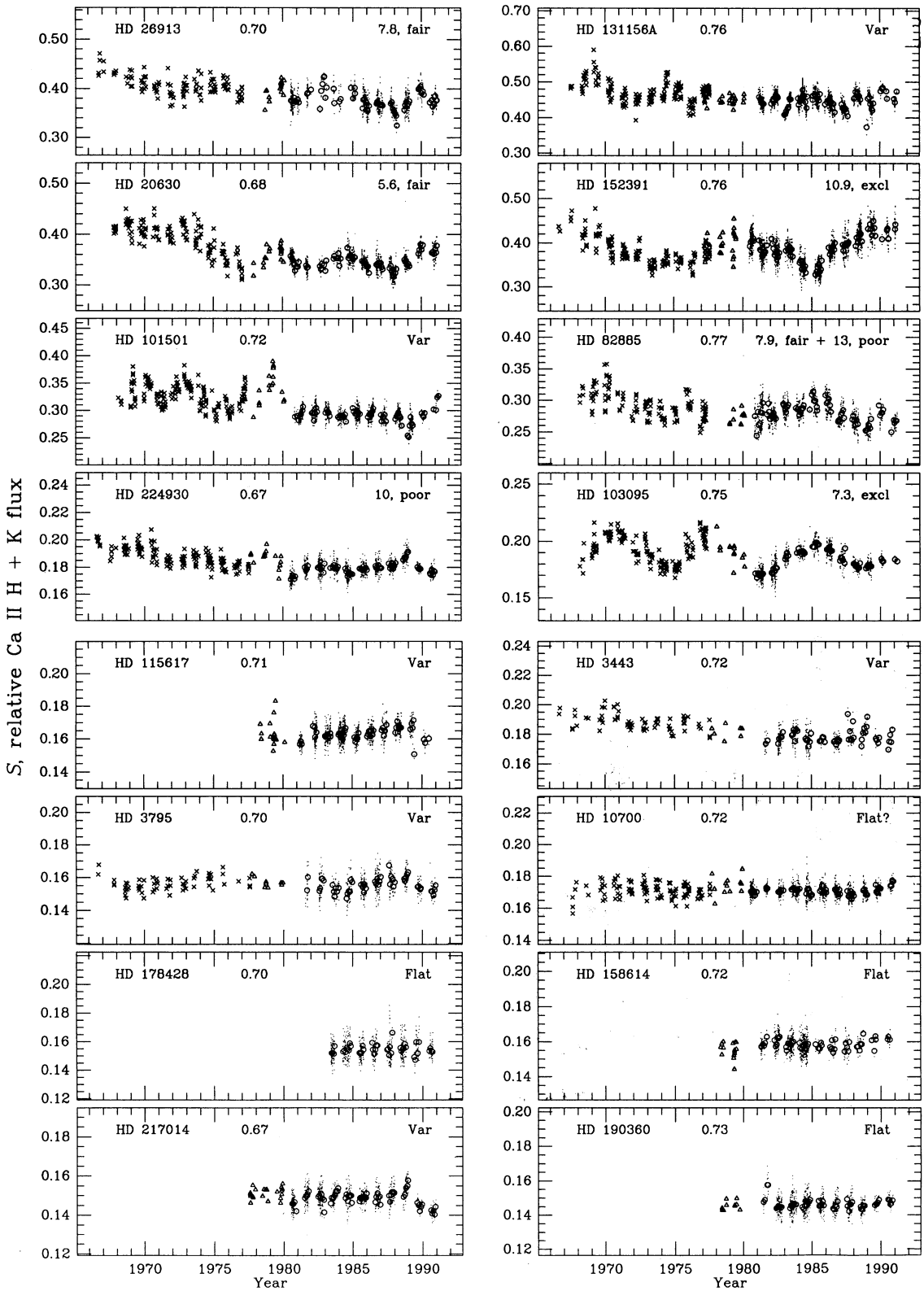

FIG. 1*e*

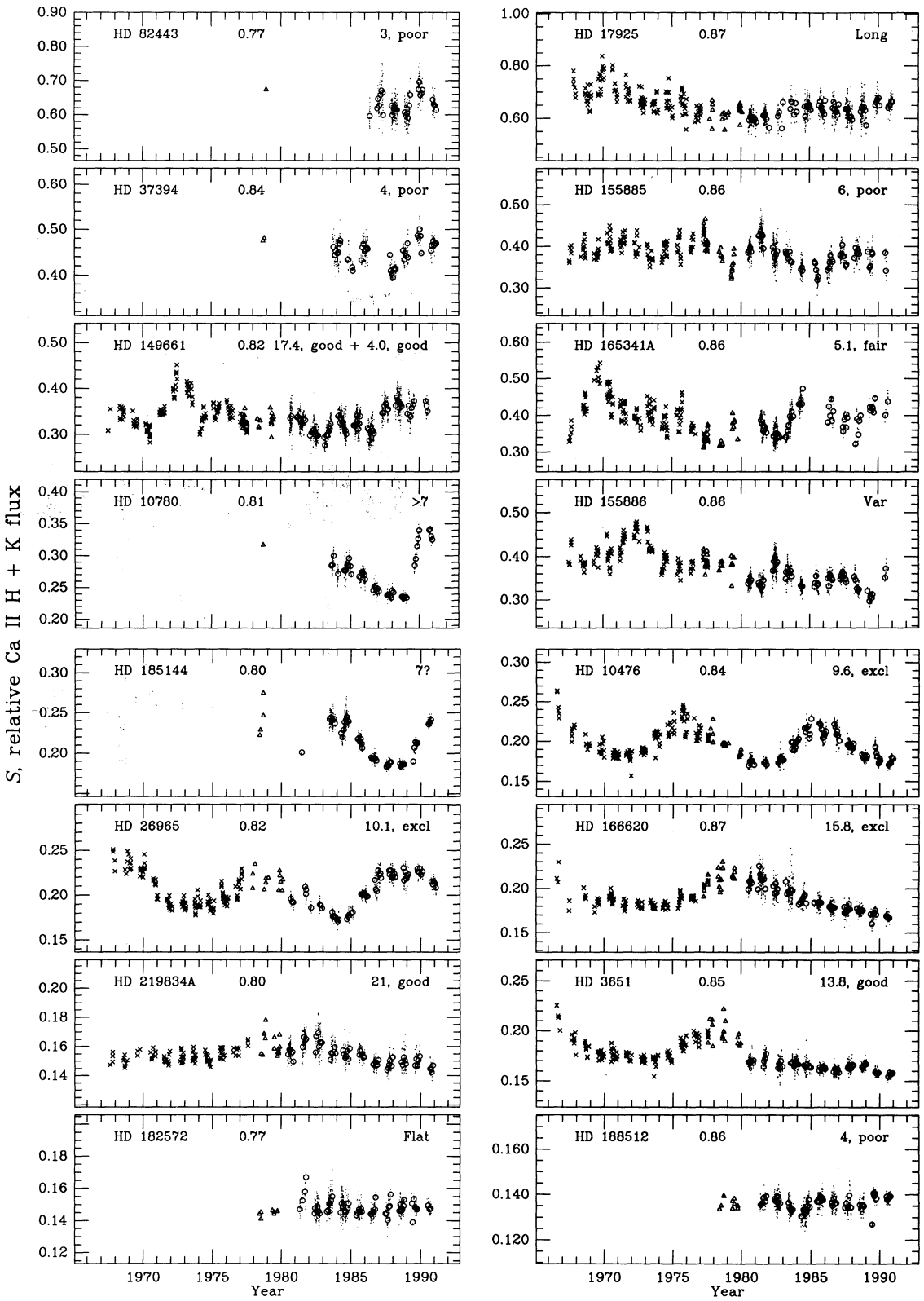

FIG. 1*f*

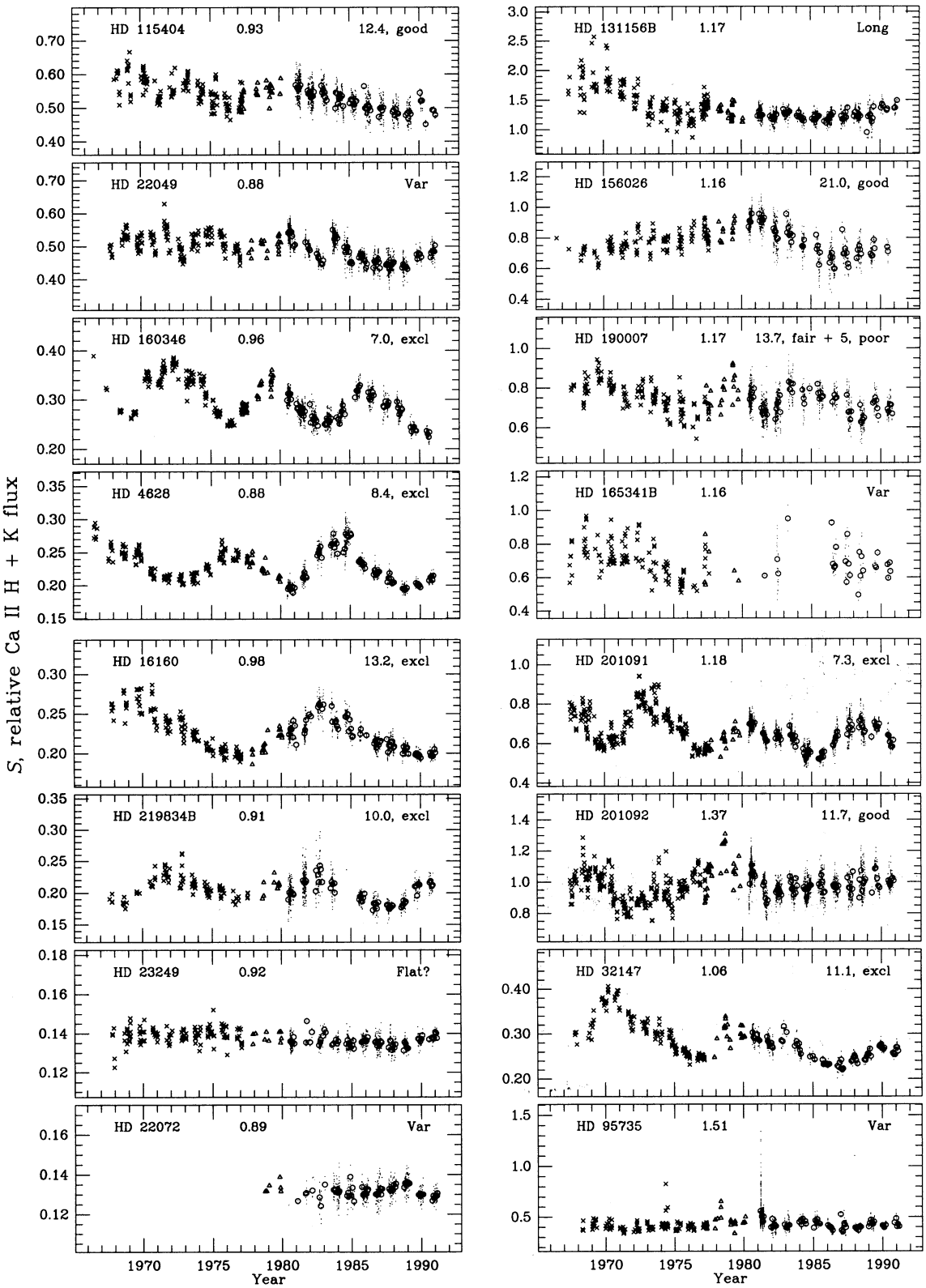

FIG. 1*g*

TABLE 2

CLASSIFICATION OF VARIABILITY IN PROGRAM STARS

HD NUMBER	STAR	FIGURE 1 REFERENCE	$B-V$	SPECTRAL TYPE[a]	$\langle S \rangle$[m]	PRIMARY CLASSIFICATION[n] $P_{cyc} \pm \Delta P$ (yr)	PRIMARY CLASSIFICATION[n] FAP Grade	SECONDARY CLASSIFICATION[o]
...	Sun	1*d*	0.66	G2 V	0.179	10.0 ± 0.1	Excellent	...
1835	9 Cet	1*d*	0.66	G2 V	0.349	$9.1^{p} \pm 0.3$	Fair	Long
2454		1*a*	0.43	F2 V	0.170	Var	...	...
3229	14 Cet	1*a*	0.44	F2 V[b]	0.224	4.9 ± 0.1	Poor	...
3443		1*e*	0.72	G5 V	0.183	Var	...	Long
3651	54 Psc	1*f*	0.85	K0 V	0.176	$13.8 \pm 0.4^{p,q}$	Good	Long
3795		1*e*	0.70	G3 V	0.156	Var	...	...
4628		1*g*	0.88	K4 V	0.230	8.37 ± 0.08	Excellent	...
6920	44 And	1*c*	0.60	F8 V	0.194	Var	...	...
9562		1*d*	0.64	G2 V[b]	0.136	Long	...	...
10476	107 Psc	1*f*	0.84	K1 V	0.198	9.6 ± 0.1	Excellent	...
10700	τ Cet	1*e*	0.72	G8 Vp	0.171	Flat ?[r]	...	...
10780		1*f*	0.81	K0 V[c]	0.280	$>7^{s}$	...	...
12235	112 Psc	1*d*	0.62	G1 V[b]	0.160	Var	...	...
13421	64 Cet	1*c*	0.56	F8 V[b]	0.131	Flat	...	...
16160		1*g*	0.98	K3 V	0.226	13.2 ± 0.2	Excellent	...
16673		1*b*	0.52	F8 V	0.215	Var	...	...
17925		1*f*	0.87	K0 V	0.653	Long	...	...
18256	ρ^3 Ari	1*a*	0.43	F5 V	0.185	6.8 ± 0.2	Fair	...
20630	κ Cet	1*e*	0.68	G5 V	0.366	$5.6^{p} \pm 0.1$	Fair	Long
22049	ϵ Eri	1*g*	0.88	K2 V	0.496	Var	...	Long
22072		1*g*	0.89	G7 V[b]	0.131	Var	...	...
23249	δ Eri	1*g*	0.92	K0 IV[d]	0.137	Flat?	...	...
25998	50 Per	1*a*	0.46	F7 V	0.300	Long	...	...
26913	V891 Tau	1*e*	0.70	G8 V[e]	0.396	$7.8^{p} \pm 0.2$	Fair	Long
26923	V774 Tau	1*c*	0.59	G0 V[b,e]	0.287	Var	...	...
26965	o^2 Eri	1*f*	0.82	K1 V	0.206	10.1 ± 0.1	Excellent	...
29645		1*c*	0.57	G3 V	0.140	Long	...	...
30495	58 Eri	1*d*	0.63	G1 V	0.297	Var	...	...
32147		1*g*	1.06	K5 V	0.286	11.1 ± 0.2	Excellent	Long
33608		1*a*	0.46	F6 V	0.214	Long	...	...
35296	111 Tau	1*b*	0.53	F8 V	0.332	Long	...	...
37394		1*f*	0.84	K1 V	0.453	$3.6^{s} \pm 0.1$	Poor	...
39587	χ^1 Ori	1*c*	0.59	G0 V	0.325	Var	...	Long
43587		1*d*	0.61	G0 V	0.156	Flat?	...	...
45067		1*c*	0.56	F8 V	0.141	Flat	...	...
61421	α CMi	1*a*	0.42	F5 IV–V	0.171	Var	...	...
72905	π^1 UMa	1*d*	0.62	F7 V	0.367	Var	...	...
75332		1*b*	0.49	F7 V	0.279	Var	...	...
76151		1*d*	0.67	G3 V	0.246	$2.52^{p} \pm 0.02$	Fair	Long
76572	61 Cnc	1*a*	0.43	F3 V	0.148	7.1 ± 0.2	Poor	...
78366		1*c*	0.60	G0 V	0.248	12.2 ± 0.4	Good	5.9 ± 0.1, fair
81809		1*d*	0.64	G2 V	0.172	8.17 ± 0.08	Excellent	...
82443		1*f*	0.77	K0 V[f]	0.635	$2.8^{s} \pm 0.1$	Poor	...
82885	11 LMi	1*e*	0.77	G8 IV–V[d]	0.284	7.9 ± 0.2	Fair	12.6 ± 0.7, poor
88355	34 Leo	1*a*	0.46	F6 V	0.170	Var	...	...
88737		1*b*	0.56	F5 V[g]	0.234	24?	...	...
89744		1*b*	0.54	F6 V	0.137	Flat	...	...
95735	Lld 21185	1*g*	1.51	M2.1 Ve[h]	0.424	Var	...	...
97344		1*d*	0.61	G0 V	0.335	Var	...	...
100180	88 Leo	1*c*	0.57	F7 V	0.165	3.56 ± 0.04	Fair	12.9 ± 0.5, fair
100563	89 Leo	1*a*	0.46	F5 V	0.202	Var	...	...
101501	61 UMa	1*e*	0.72	G8 V	0.311	Var	...	Long
103095	Gmb 1830	1*e*	0.75	G8 VI	0.188	7.30 ± 0.08	Excellent	...
106516		1*a*	0.46	F6 V	0.208	Var	...	...
107213	9 Com	1*b*	0.50	F8 V	0.135	Long	...	...
111456		1*a*	0.46	F6 V	0.300	7[s]?	...	...
114378	α Com	1*a*	0.45	F5 V + F5 V	0.244	Long	...	...
114710	β Com	1*c*	0.57	G0 V	0.201	16.6 ± 0.6	Good	9.6 ± 0.3, fair
115043		1*c*	0.60	G1 V[f]	0.327	Var	...	...
115383	59 Vir	1*c*	0.58	F8 V	0.313	Var	...	...
115404		1*g*	0.93	K1 V[f]	0.535	12.4 ± 0.4	Good	...
115617	61 Vir	1*e*	0.71	G6 V	0.162	Var	...	...
120136	τ Boo	1*b*	0.48	F7 V[b]	0.191	11.6 ± 0.5	Poor	...
124570	14 Boo	1*b*	0.54	F6 V[b]	0.133	Flat	...	...
124850	ι Vir	1*b*	0.52	F7 IV[i]	0.210	Long	...	...
126053		1*d*	0.63	G3 V	0.165	22?	...	...
129333	EK Dra	1*d*	0.61	G0 V[j]	0.544	Var	...	...

TABLE 2—*Continued*

HD Number	Star	Figure 1 Reference	$B-V$	Spectral Type[a]	$\langle S \rangle^m$	Primary Classification[n] $P_{cyc} \pm \Delta P$ (yr)	FAP Grade	Secondary Classification[o]
131156A	ξ Boo A	1*e*	0.76	G8 V	0.461	Var	...	...
131156B.....	ξ Boo B	1*g*	1.17	K4 V	1.381	Long	...	...
136202	5 Ser	1*b*	0.54	F8 IV–V[k]	0.140	Long	...	...
137107AB.....	η CrB	1*c*	0.58	G2 V + G2 V	0.184	Var	...	...
141004	λ Ser	1*d*	0.60	G0 V	0.155	Long	...	...
142373	χ Her	1*c*	0.56	F9 V	0.147	Flat	...	...
143761	ρ CrB	1*d*	0.60	G2 V	0.150	Long	...	...
149661	12 Oph	1*f*	0.82	K0 V	0.339	17.4 ± 0.7	Good	4.00 ± 0.04, Good
152391		1*e*	0.76	G7 V[f]	0.393	10.9 ± 0.2	Excellent	...
154417		1*c*	0.57	F8 V[b]	0.269	7.4 ± 0.2	Fair	...
155885	36 Oph B	1*f*	0.86	K1 V	0.384	5.7 ± 0.1	Poor	...
155886	36 Oph A	1*f*	0.86	K0 V	0.375	Var	...	Long
156026		1g	1.16	K5 V[f]	0.770	21.0 ± 0.9	Good	...
157856		1*a*	0.46	F5 V[g]	0.202	15.9 ± 0.8	Fair	...
158614		1*e*	0.72	G8 IV–V	0.158	Flat	...	...
159332		1*b*	0.48	F4 V	0.144	Flat?	...	...
160346		1*g*	0.96	K3 V[f]	0.300	7.00 ± 0.08	Excellent	...
161239	84 Her	1*d*	0.65	G6 V[l]	0.138	5.7 ± 0.1	Fair	11.8 ± 0.5, poor
165341A	70 Oph A	1*f*	0.86	K0 V	0.392	5.1 ± 0.1	Fair	...
165341B.....	70 Oph B	1*g*	1.16	K6 V	0.691	Var	...	...
166620		1*f*	0.87	K2 V	0.190	15.8 ± 0.3	Excellent	...
176051		1*c*	0.59	G0 V	0.176	10[s]?	...	...
176095		1*a*	0.46	F5 IV[j]	0.202	Long	...	...
178428		1*e*	0.70	G4 V	0.154	Flat	...	...
182101		1*a*	0.44	F6 V	0.216	5.1 ± 0.1	Poor	...
182572	31 Aql	1*f*	0.77	G8 IV	0.148	Flat	...	...
185144	σ Dra	1*f*	0.80	K0 V	0.215	7[s]?	...	...
187013	17 Cyg	1*b*	0.47	F5 V	0.154	Long	...	...
187691	*o* Aql	1*b*	0.55	F8 V	0.148	5.4 ± 0.1	Fair	...
188512	β Aql	1*f*	0.86	G8 IV[d]	0.136	4.1[s] ± 0.1	Poor	...
190007		1*g*	1.17	K4 V[j]	0.746	13.7 ± 0.7	Fair	5.3 ± 0.1, poor
190360		1*e*	0.73	G6 IV[d]	0.146	Flat	...	...
190406	15 Sge	1*d*	0.61	G1 V	0.194	2.60 ± 0.02	Fair	16.9 ± 0.8, good
194012		1*b*	0.51	F5 V[j]	0.198	16.7 ± 0.9	Poor	5.4 ± 0.1, fair
201091	61 Cyg	1*g*	1.18	K5 V	0.658	7.3 ± 0.1	Excellent	...
201092		1*g*	1.37	K7 V	0.986	11.7 ± 0.4	Good	...
206860	HN Peg	1*c*	0.59	G0 V	0.330	6.2 ± 0.2	Poor	...
207978	15 Peg	1*a*	0.42	F0 V[b]	0.152	Flat	...	...
212754	34 Peg	1*b*	0.52	F5 V	0.140	Long	...	...
216385	σ Peg	1*b*	0.48	F7 IV	0.142	Flat	...	...
217014	51 Peg	1*e*	0.67	G5 V[b]	0.149	Var	...	...
219834A	94 Aqr A	1*f*	0.80	G5 IV–V	0.155	21 ± 1	Good	...
219834B.....	94 Aqr B	1*g*	0.91	K2 V	0.204	10.0 ± 0.2	Excellent	...
224930	85 Peg	1*e*	0.67	G3 V	0.184	10.2[p] ± 0.4	Poor	Long

NOTE.—Variability classification: "Var" means significant variability without pronounced periodicity, on timescales longer than 1 yr but much shorter than 25 yr ($\langle \sigma_S/S \rangle \gtrsim 2\%$). "Flat" means $\langle \sigma_S/S \rangle < 1\%$–$1.5\%$. "Flat?" means $\langle \sigma_S/S \rangle \approx 1.5\%$–$2\%$. "Long" means significant variability on timescales longer than 25 yr. Note that some records show secular change over 25 yr which suggests that, if present, cycle period > 50 yr.

[a] Spectral type except for Sun from Third Edition of the Catalogue of Bright Stars (Hoffleit 1964) unless otherwise noted. Spectral type and $B-V$ for the Sun from Keenan 1991 and Hardorp 1980, respectively.

[b] Spectral type from Fifth Edition of the Catalogue of Bright Stars (Hoffleit & Warren 1991) indicates that luminosity class may be IV or IV–V.

[c] Listed erroneously in Fifth Edition as M1 III.

[d] Absolute magnitude determined from the width of the Ca II lines (Wilson 1976) confirm that star is above the main sequence.

[e] Soderblom & Mayor 1993 list the spectral types for HD 26913 and HD 26923 as G8 V and G0 V, respectively, as observed by Slettebak 1963. Stephenson 1960 observed them as G5 IV + G0 IV, but Wilson & Skumanich 1964 observations of Sr II λ4077 place them firmly on the main sequence.

[f] Spectral type from A Supplement to the Bright Star Catalogue (Hoffleit, Saladyga, & Wlasŭk 1983).

[g] Buscombe 1980.

[h] Buscombe 1984.

[i] Wilson 1984 finds no Ca II emission, and Sr II λ4077 comparable in strength to Fe I λ4063. Doubtful that it is F6 III as listed in Fifth Edition.

[j] Buscombe 1977.

[k] Listed in Fifth Edition as F8 III–IV; 10 Å mm^{-1} spectra preclude it being III.

[l] On 10 Å mm^{-1} spectrograms obtained by Wilson prior to the beginning of the survey, the intensity of Sr II λ4077 is much weaker than that of Fe I λ4063 (Wilson 1984). Thus, the star is less luminous than class III as listed in both the Fourth and Fifth Editions of the Catalogue of Bright Stars.

[m] Annually averaged mean over all years.

[n] If cyclic, period P_{cyc}, $\pm\Delta P$, and FAP (in percent) grade are listed as excellent $\equiv FAP \leq 10^{-9}$, good $\equiv 10^{-9} < FAP \leq 10^{-5}$, fair $\equiv 10^{-5} < FAP \leq 10^{-2}$, and poor $\equiv 10^{-2} < FAP \leq 10^{-1}$.

[o] Secondary period present in the periodogram after the primary frequency was filtered out, or behavior on timescales >25 yr.

[p] Linear trend removed prior to period identification.

[q] Maunder-minimum activity beginning after 1980?

[r] Possible increasing activity after 1988.

[s] Sparse data prior to 1980, not included in periodogram analysis.

purely Gaussian noise:

$$FAP = 100[1 - (1 - e^{-z/\sigma^2})^{N_i}] , \quad (2)$$

where σ^2 is the total variance of the data and N_i is the number of independent frequencies, which are estimated using the prescription outlined by Horne & Baliunas (1986). In this paper, we define the cutoff in *FAP* for the detection of a periodicity to be 0.1%, or a 99.9% confidence level that the peak is not caused by Gaussian noise.

This apparently high confidence level for our cutoff arises because the methodology has shortcomings in application to our data series. The methodology assumes the signal consists of one or more pure sinusoids plus Gaussian noise. The normalized periodogram analysis yields the best sinusoid that fits the unevenly sampled data, and the significance of the period is inferred from its false alarm probability. But the existence of a peak can be biased by effects not included in the formal computation of the false alarm probability, which in our case can yield correct relative rankings, but inflated confidence levels.

Biases may be introduced by additional time-dependent stellar phenomena which can contribute to the power near a particular frequency. However, the records often contain variations that are neither sinusoidal nor Gaussian noise. Most importantly, the number of cycles contained in the length of the time series is generally small. A transient variation could dramatically increase the power at a particular frequency without representing a repetitive phenomenon. For example, the growth and decay of active regions responsible for the emission is "stellar noise" that is not Gaussian and may alter the frequency of a peak or the height of a peak or result in two apparent peaks in the power spectrum (and give the incorrect perception of two independent frequencies in the power spectrum; Horne & Baliunas 1986). Without knowledge of the lifetimes of the emitting areas, it is difficult to correct for active region evolution. Gilliland & Baliunas (1987) attempted to refine the cycle analysis by attempting to correct stellar data for the finite lifetimes of active regions. The calculation of the pooled variance on different timescales (Dobson et al. 1990; Donahue 1993) can also be used as a technique for estimating the timescales over which active region evolution makes the greatest contribution. Unfortunately, the timescales of particular interest, 50–300 days, are severely undersampled because of the seasonal observing window. The effects of active region evolution are smallest in the cases where the activity cycle amplitude is large, or when the activity cycle period is far from the timescale for which active region growth and decay is the most evident.

For all these reasons the confidence level of the *FAP* cannot be taken too literally. We have rescaled the confidence levels to relative grades ("poor" to "excellent"; see note to Table 2) based on the estimate of uncertainties cited above and the visual appearance of the records.

We also estimate the uncertainty in the calculation of the detected peak, ΔP (Kovács 1981; Baliunas et al. 1985; Horne & Baliunas 1986):

$$\Delta P = \frac{3\sigma_n P_{\rm cyc}^2}{4TA\sqrt{N}} , \quad (3)$$

where σ_n^2 is the variance of the noise *after* the subtraction of the observed periodic signal (which should not be confused with the total variance, σ^2, used in the computation of the false alarm probability in eq. [2]), N is the number of data points, T is the total length of the observing interval, and A is the amplitude of the signal. The values of A and σ_n^2 are calculated from the least-squares fit to the data of a sinusoid whose frequency corresponds to the significant peak in the periodogram. After subtracting this fitted sinusoid from the data, we computed the variance of the noise, σ_n^2, from the residuals.

In addition, we note that ΔP is *not* the accuracy of the period, because $P_{\rm cyc}$ itself can vary. For example, the period of the sunspot cycle determined within 20 yr intervals varies from 9 to 13 yr over the last 250 yr (Donahue & Baliunas 1992a). In fact, the measured period for the Sun based on the recent 25 yr chromospheric record is 10.0 yr, over 10% smaller than the mean 11 yr period that has been observed over a much longer baseline.

The classifications of the long-term variability that result from this analysis are shown in the panel for each record in Figure 1 and are listed in Table 2. A few stars show multiple periods or trends superposed on other variations. These are noted in the column labeled "Secondary Classification" in Table 2. Multiple periods were determined to be present when a significant residual peak was detected in the periodogram after the primary frequency was filtered from the time series (Baliunas et al. 1985). Filtering the first period out alters the interpretation of the power spectrum for any residual peak, since the variance of the data has been changed. The values of ΔP and the false alarm probability from the revised periodogram will still be valid, provided that the initial period determination is correct.

The amplitude and timescale of variations are the fundamental assessments of activity variability, which may not be periodic. Our determination of the existence of a cycle has important limitations when the interval of observation is short and when variability occurs on timescales longer than the measurement window. The detection of cycles greater than 25 yr requires longer intervals of observation. For example, photometric measurements of the dK5e star BD +26°730 (Hartmann et al. 1981) show a cycle on the order of 60 yr.

4. RESULTS

The classifications of the chromospheric emission records are summarized in Figures 2 and 3. Figure 2 shows log $\langle S \rangle$ as a function of the $(B-V)$ color index, which is roughly equivalent to age or rotation as a function of mass on the lower main sequence. The plotted symbol for each star denotes the classification of dominant variations measured over the 25 yr interval. Figure 3 is a histogram of the classes in Figure 2 and includes the distribution of cycle periods.

4.1. *Comments on Cycle Classification*

The sample in the log $\langle S \rangle$ versus $(B-V)$ plane (Fig. 2) is roughly divided into two groups with the division roughly along the diagonal line, as first noted by Vaughan & Preston (1980) from their larger solar neighborhood survey. The stars in the upper region of the diagram tend to have higher $\langle S \rangle$, more rapid rotation, and therefore younger main-sequence ages. The stars in the lower region (including the Sun) have lower $\langle S \rangle$, slower rotation, and greater ages.

The ratio S is sensitive to stellar photospheric temperature and is the primary cause for the tendency of $\langle S \rangle$ to increase as $(B-V)$ increases. Color corrections for S and possible interpretations in terms of theoretical or model-dependent parameters have been previously discussed (Middlekoop 1982; Noyes et al. 1984; Rutten 1984). Since the primary focus of this paper is the

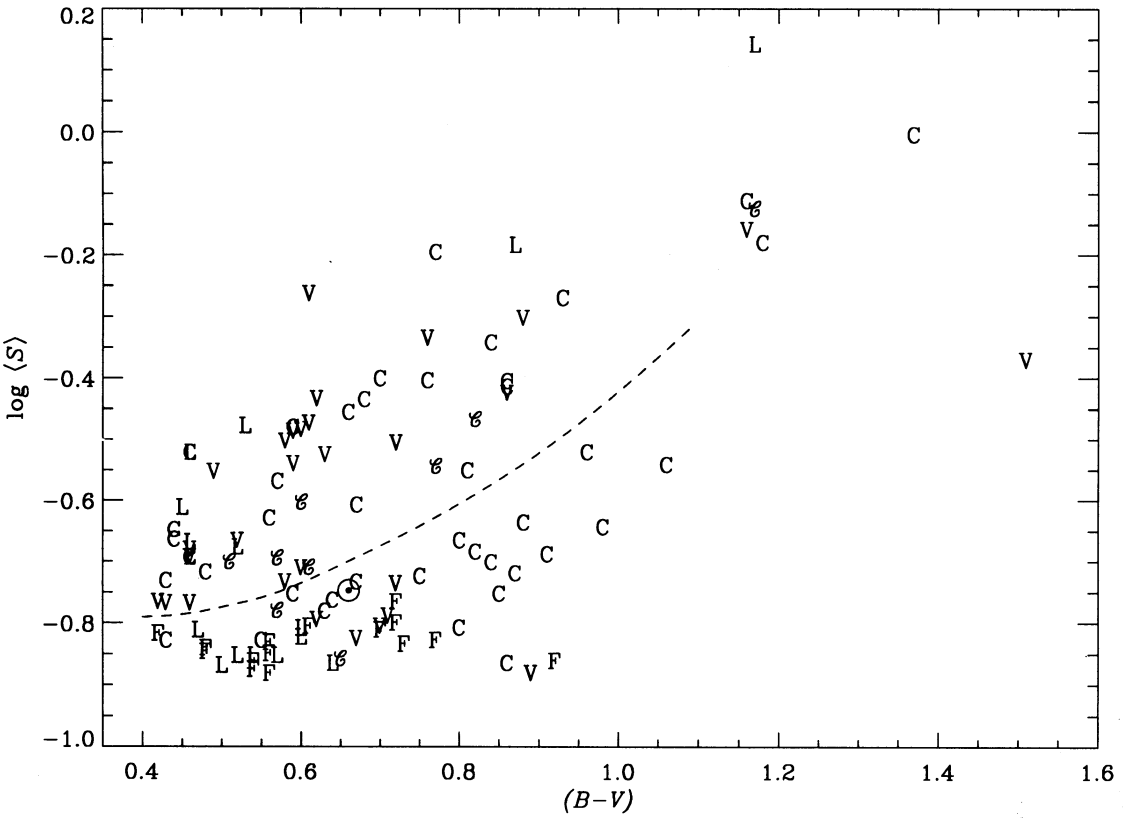

FIG. 2.—The distribution of chromospheric activity with $B-V$ (roughly equivalent to mass in lower main-sequence stars) along with long-term variability classification. Stars with "C" classifications have measured activity cycle periods; those labeled "𝒞" have secondary periods. Stars labeled "V" have variable activity with no clear period; "L" means long-term trend; "F" means flat with little or no change in activity (see Table 2). The positions of the Sun (⊙) is also marked. The dashed line roughly separates the stars with high or low $\langle S \rangle$.

presentation of the measurements, we will defer a discussion of parameterizations of S to a subsequent paper.

Figure 2 reveals some aspects of the chromospheric emission variability that depend on stellar mass and age. For example, K-type stars with low $\langle S \rangle$ values almost all have pronounced cycles. The exception is the subgiant HD 23249 (δ Eri) and therefore not comparable to the dwarf stars.

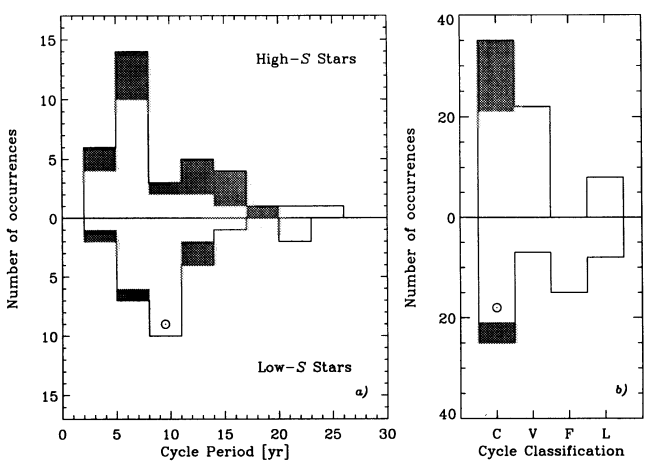

FIG. 3.—(*a*) The distribution of cycle periods (in 3 yr bins) for high-$\langle S \rangle$ (*upper histogram*) and low-$\langle S \rangle$ (*lower histogram*) stars (see text). Shaded areas represent secondary periods for stars where two periods were measured. The ⊙ symbol indicates the bin containing the Sun. (*b*) Similar to (*a*) except that the distribution of long-term activity classifications are shown: "C" cyclic (the shaded area shows additional secondary cycle periods), "V" variable, "F" flat (nonvarying), and "L" long-term trend.

F-type stars, especially those stars with low $\langle S \rangle$, generally have nearly constant records (*flat*) or slow, secular variations (*long*). Variability in that region of the diagram is difficult to detect, certainly in part because of the weakness of chromospheric emission and its low contrast relative to the photospheric flux, but possibly also because cyclic variability with significant amplitudes does not occur among those stars. The F-type stars have shallow convective zones and relatively rapid rotation compared to the Sun, which may produce activity variations that differ significantly from the Sun's.

Among the G-type stars, very low amplitudes of chromospheric variation and levels of activity occur only in stars with low $\langle S \rangle$. Such low activity and flat variability may be similar to episodes of low magnetism such as the Maunder Minimum[23] of the seventeenth century (Eddy 1976; Damon 1977). The Sun and stars with *flat* records have slow rotation and are therefore old, suggesting that the Maunder minimum phase appears in old stars. However, great age per se cannot explain chromospheric inactivity in the Maunder minimum stars (see Appendix A) for four reasons. First, the Sun shows a range of chromospheric activity, including occasional Maunder minimum phases; second, HD 3651 appears to have

[23] In this paper we distinguish between the historical "Maunder Minimum" of the Sun, and the generalization of the term "Maunder minimum" to include all sustained lulls in chromospheric activity (Baliunas & Jastrow 1990).

been observed entering a Maunder minimum phase; third, HD 9562 is slightly younger than the Sun yet is much less active than the Sun; and fourth, HD 103095 is a very old star with pronounced cyclic variations. The Maunder minimum appears to be a *temporary* phenomenon between phases of cyclic activity and *not* inactivity due to advanced age.

A few stars of all spectral types have two significant cycles. Those stars are located at intermediate values of $\langle S \rangle$, and are close to the Vaughan-Preston gap. The location of that group of double-period stars (Fig. 2) suggests that the gap may have physical significance and is not an artifact of the selection of the sample.

Stars with significant variability and no preferred timescale (*var*) are generally young. Such activity records may result from the superposition of several weak periods which are unresolved in the 25 yr observing interval, or from nonperiodic variations.

Figure 3 is a histogram of the classification shown in Figure 2 and includes the distribution of cycle periods. Both periods are shown for stars with dual activity cycles. Roughly 52 stars (including the Sun) show cycles, 31 are flat or have linear trends over the observing interval, and 29 show variability with no periodicity. Of the stars with cycles, measured periods range from 2.5 yr to at least the length of the interval of observations, 25 yr. No period with a grade of "good" or "excellent" is shorter than 7 yr, although the measurements would reveal such short periods if they existed. Nor does the Sun show any cycle shorter than 7 yr over the past 250 yr (Eddy 1977; Donahue & Baliunas 1992a). One interpretation of the existence of a cutoff at short cycle periods is that the mechanism that produces the activity cycle operates over a timescale of at least 7 yr. The short periods that are observed generally have confidence levels worse than in the good-to-excellent group. The existence of short but weak cycles might suggest that they are unstable and do not persist over the 25 yr interval of observations and are more common among stars with high $\langle S \rangle$ values.

4.2. *Evolution of Activity*

The average level of chromospheric activity and rotation both change on an evolutionary timescale (e.g., Wilson 1963, 1966; Kraft 1967; Skumanich 1972). Figure 2 suggests that the pattern of time variation of activity also changes on evolutionary timescales as angular momentum is lost. By considering stars close in color to avoid the bias of photospheric temperature in $\langle S \rangle$, we can trace the evolution of a specific type of star. For example, the young Sun (as in HD 129333 = EK Dra) should have had a high $\langle S \rangle$, rapid rotation, no Maunder minimum phase, and only a rare occurrence of a smooth cycle. At an intermediate age (as in HD 114710 = β Com), the Sun should have had moderate $\langle S \rangle$ and rotation, with occasional smooth cycles compared to the present Sun. At the current age of the Sun and older, rotation is slow, $\langle S \rangle$ is lower, and cycles are smooth (as in HD 81809), and occasionally suppressed (as in HD 9562).

4.3. *Visual Binaries*

The visual binaries (HD 26913/23, 131156A/B, 155885/6, 165341A/B, 201091/2, 219834A/B) are pairs of presumably coeval stars for which the factor of age is controlled. The stars HD 155885/6 are very close in spectral type (i.e., mass) and rotation; thus, the differences in their chromospheric records are presumably due to the limited interval of measurement which reveals different phases of longer-term variations. The older stars HD 219834A/B, although somewhat different in spectral type, both show cyclic activity.

4.4. *Asymmetry of Slopes Computed over 25 Years*

A histogram of the slopes of linear fits of the entire record for each star shows a distribution around a maximum occurrence at zero slope that is slightly asymmetric, with the larger tail toward negative slopes. The asymmetry in the distribution may be caused by an activity variation whose shape is a quick rise followed by a slow decline, as is often the case for the Sun (Waldmeier 1961). A long-term drift in the instrumental calibration cannot explain the asymmetric distribution of slopes, because several stars that have low variability and were not used as standards in the calibration procedure, e.g., HD 10700, show no significant trend.

5. DISCUSSION

As Wilson's work indicated, the variability of stellar activity in general is richer than the Sun's variability, despite the limited interval of the stellar observations compared to the solar records. The 25 yr records of similar stars can be considered as an ensemble of variations occurring on much longer timescales, i.e., centuries. Two examples are HD 3651, which may have entered the Maunder minimum phase, and HD 10700, which may have begun to emerge from the Maunder minimum phase starting in 1990. Compared to Wilson's records, the longer interval of observations shown here allows us to measure stellar cycles with periods up to 25 yr that could not be measured in a shorter time. Another benefit of the extended period of observation is a better definition of the average timescale and amplitude of variability of short periods, as well as their deviations.

Still longer intervals of observations may resolve the records of those stars with activity variations that are substantial but not periodic. Such variations may be multiply periodic on timescales of many decades. In addition, better statistics from extended observations of stars with short-period variations may reveal occasional, as opposed to persistent, periodicity and may explain why the short cycle periods such as for HD 190406 are of lower confidence levels in the 25 yr record of higher confidence in shorter intervals.

The year 1996 marks the centennial of the casting of the 60 inch mirror, which was a gift to George Ellery Hale from his father. Hale (1915) thought the great reflector could be used in "studies of physical condition and of evolutional progress in which we hoped to aid in tracing the life-history of stars and systems from their birth to their decay."

We are saddened by the deaths of our colleagues, Alain Porter and Olin C. Wilson.

We thank S. Keil for the SPO solar data and W. C. Livingston and O. R. White for the KPNO solar data. We also thank P. Cronin, R. Eklund, D. Mihalas, E. N. Parker, F. Perez, L. Webster, and L. Widrow for their invaluable advice and assistance. This research was supported by the Mobil Foundation, Inc.; the Carnegie Institution of Washington; the Richard Lounsbery Foundation; the Scholarly Studies Program, Langley-Abbot, and James Arthur funds of the Smithsonian Institution; the National Aeronautics and Space Administration (NSG 07148); the National Science Foundation (AST 79-21070, AST 81-21726, AST 86-16545); the National Geographic Society (2548-82); the Department of Energy grant

DE-AC02-76ER03075; the American Petroleum Institute; the Electric Power Research Institute; the National Coal Association; the American Railroad Institute; the Edison Electric Institute; the Texaco Foundation, Inc., as well as several generous individuals. The observations contained in this research since 1989 were made possible by an agreement between Mount Wilson Institute and the Carnegie Institution of Washington.

APPENDIX A

INDIVIDUAL STARS

The activity records of a few stars warrant detailed comments.

HD 3651 (*= 54 Psc K0 V*).—This star has gradually decreased in chromospheric activity since it was first observed. The most recent activity maximum (circa 1989) is extraordinarily low compared to maximum in 1978 and the observations in 1966 which appear to have occurred near or just after an activity maximum. The change in amplitude of the activity cycle over several decades suggests that the star is entering a period of low-amplitude variation, similar to the solar Maunder Minimum (Eddy 1976; Baliunas & Jastrow 1990).

HD 9562 (*G2 V*).—This star has a flat activity record, yet $v \sin i$ is 2–3 km s^{-1} (Saar 1994), suggesting that the rotation period is shorter than the Sun's 25 days and that it is slightly younger than the Sun. Its $\langle S \rangle$ is about 20% lower than the Sun's. The relative inactivity in HD 9562 for its rotation implies a Maunder minimum phase.

HD 10700 (*= τ Cet, G8 Vp*).—Most stars redder than $(B-V) = 0.6$, or later than spectral type G0 V, show significant long-term fluctuations. An exception is HD 10700, which has a standard deviation of 1.2%, one of the smallest standard deviations of any star in the survey except the standard stars. The low amplitude suggests that HD 10700 may be in a Maunder minimum state. After 1989, chromospheric activity increases slightly, perhaps signaling a return to a phase of cyclic activity. The star is slightly metal deficient, with [Fe/H] $\lesssim -0.13$ (e.g., Soon et al. 1993). The observed $v \sin i$ is <1 km s^{-1} (Saar 1994), which suggests a rotation period of $\lesssim 45$ days; however, $\langle S \rangle$ is 0.171 implying an estimated rotation period of 32 days (Noyes et al. 1984). If the star is in or near a Maunder minimum phase, the estimates of rotation period from its mean chromospheric activity and measured $v \sin i$ can be reconciled only if the star is highly inclined.

HD 10780 (*K0 V*).—This star shows the largest intraseasonal change in chromospheric activity. During the 1989–1990 observing season, S increased by $>25\%$.

HD 81809 (*G2 V*).—This star has previously been described as a twin to the Sun since it has similar $(B-V)$ color, mean level of chromospheric activity, and has an activity cycle period (8 yr) just on the edge of the range of observed sunspot cycle lengths (Eddy 1977; Donahue & Baliunas 1992a). The peculiarity lies in its 40 day rotation period (Noyes et al. 1984) which implies either great age (which is inconsistent with the mean S-value) or lower mass (inconsistent with the color index). However, the star is a binary (see Appendix B), and the observed activity may arise from the lower mass component, whose spectral type can be estimated from the rotation period to be K0 V. The apparent smoothness of the 8.17 yr activity cycle and seasonal rotation data suggests that the primary is a much less active star and perhaps near G0 spectral type in order to produce the combined type of G2 V.

HD 95735 (*= Lalande 21185, M2.1 V*).—This star is the coolest star in the survey. Although it is quiet compared to the dMe flare stars, we have observed several flares. One spectacular flare occurred in 1981, when S was first observed at a value of nearly 1.5 and then decayed over a 2 hr period (Donahue et al. 1986).

HD 103095 (*= Groombridge 1830, G8 VI*).—This star is the sole Population II star in the survey. Despite its age (≥ 10 Gyr; Smith, Lambert, & Ruck 1992), and weak metal abundance ([Fe/H] $\lesssim -1.0$; Soon et al. 1993), it still has a noticeable 7.3 yr activity cycle, demonstrating that old, metal-deficient stars can support vigorous activity cycles.

HD 114710 (*= β Com, G0 V*).—This star is similar to the Sun at an age of ~ 2 Gyr. It has a 16.6 yr activity cycle superposed on a 9.6 yr cycle. The appearance of two cycles occurs in stars near the Vaughan-Preston gap, as noted above (§ 4.1). The observed rotation changes with phase of activity cycle and may indicate the presence of surface differential rotation (Donahue & Baliunas 1992b).

HD 129333 (*= EK Dra, G0 V*).—This star is one of the youngest (0.07 Gyr; Dorren & Guinan 1994) and most active G stars in the survey.

HD 131156B (*= ξ Boo B, K4 V*).—This star has the largest amplitude of chromospheric activity observed. Since observations began in 1967, S decreased from ~ 2.1 to a minimum of $S \sim 1.2$ circa 1984, then increased, although a single cycle is not yet complete.

HD 141004 (*= λ Ser, G0 V*).—This star has rotation (26 days) and mass similar to the Sun, but weak chromospheric activity, and a variation in activity that appears to be longer than 30 yr in length.

HD 142373 (*= χ Her, F9 V*).—This star has the lowest value of $\sigma_S/\langle S \rangle$ in the survey, 0.8% (Table 1); the low variability indicates the long-term stability of the instrument.

HD 161239 (*= 84 Her, G6 V*).—This star has one of the weakest activity levels observed ($\langle S \rangle = 0.138$) but detectable variation. This might suggest that this star is actually an undetected binary or that it is slightly evolved.

HD 190406 (*= 15 Sge, G1 V*).—This star displayed for many years one of the shortest activity cycle periods observed, 2.6 yr. That variation is most noticeable before its subsidence near 1986. After the 2.6 yr cycle is filtered, a 16.9 yr period emerges.

APPENDIX B

POSSIBLE BINARY STARS

Wilson avoided known, unresolved binaries in his monitoring program. Four complications arise from observations of such systems. First, the average level of chromospheric activity may be affected by the contribution of flux to the chromospheric and photospheric passbands from a second star. Second, both stars may vary in chromospheric flux and leave a record of superposed and inseparable variations. Third, if the system is a spectroscopic binary, radial velocity variations above several km s^{-1} will modulate the observed flux, unless the orbital velocities are corrected by repositioning the exit slit at the time of each observation. Fourth, the interpretation of activity in single stars may be obscured by the inclusion of stars in binaries.

Recent reports in the literature yield additional information on the existence of previously unknown or suspected binaries in the sample:

HD 3443.—Variations in the radial velocities of the components were determined from variations in the blended line widths. The orbital period is 25 yr, and semimajor axis, $a = 0''.67$. If the orbital inclination is 78° (van den Bos 1937), then the masses are roughly 1.10 $M_\odot$ and 0.87 $M_\odot$, which are slightly larger than expected from the spectral type (Duquennoy & Mayor 1991). Thus, the activity record may be the combined variations of both components.

HD 39587 (= χ^1 *Ori*).—Lippincott & Worth (1978) first detected this binary astrometrically. A precise orbit was determined by Irwin, Yang, & Walker (1992), with $a = 0''.082$, $M_2 \sim 0.15\ M_\odot$, and $M_V > 8.8$. Gatewood (1994) finds $a = 0''.097$. The estimated mass and observed luminosity suggest that the secondary has not reached the main sequence. The relative brightness of the primary suggests that it dominates the activity record.

HD 76572 (= *61 Cnc*).—Tokovinin & Ismailov (1988) report a separation of $0''.048$ if the components are of equal brightness. It was unresolved by Balega, Balega, & Vasyuk (1991).

HD 81809.—Radial velocity measurements suggest an orbital period of 35 yr. If $i = 82°.8$, then masses are $1.5 \pm 0.5\ M_\odot$ and $0.8 \pm 0.2\ M_\odot$, suggesting ~G0 V + K0 V; the magnitude difference in the V-passband, ΔV, is ~0.8 mag (Duquennoy & Mayor 1991). Visible measurements by Baize (1985) and speckle interferometry by McAlister, Hartkopf, & Franz (1990) observed a $0''.4$ separation.

HD 88355 (= *34 Leo*).—This star has $\Delta V \sim 0.8$ mag (Hoffleit & Jaschek 1982) and $M_1 + M_2 = 3.5\ M_\odot$ (Baize 1985). The primary may be so massive that it lacks significant Ca II variability, in which case the less-massive component produces the chromospheric variations. McAlister et al. (1990) list a $0''.124$ separation.

HD 114378 (= α *Com*).—Duquennoy & Mayor (1991) find a constant radial velocity (i.e., the system is not a spectroscopic binary). McAlister et al. (1990) measure speckle components at separations of $0''.1$ and $0''.05$ at different times. Hoffleit & Jaschek (1982) list $\Delta V \sim 0.8$ mag. The identical spectral types (Table 2) suggest that both components may contribute variability to the observed record.

HD 124570 (= *14 Boo*).—This star is listed as a single-lined spectroscopic binary (Hoffleit & Jaschek 1982); however, Morbey & Griffin (1987) find constant radial velocities. McAlister et al. (1990) list $0''.184$ separation. It was unresolved by Balega et al. (1991).

HD 137107 (= η *CrB*).—If $i \sim 58°$ (Silbernagel 1929), then $M_1 = 1.19\ M_\odot$, $M_2 = 0.98\ M_\odot$ (Duquennoy & Mayor 1991). Hoffleit & Jaschek (1982) give $\Delta V \sim 0.3$ mag. Both components are likely to contribute to the activity record.

HD 141004 (= λ *Ser*).—Although this star has been listed as a binary, Morbey & Griffin (1987) and Duquennoy & Mayor (1991) infer constant radial velocities. It was unresolved by Balega et al. (1991); the star seems not to be a binary (Heintz 1993).

HD 156026.—Although this star has been listed as a binary, it was unresolved by speckle (Blazit, Bonneau, & Foy 1987). Beavers & Eitter (1986) find constant radial velocity; the star is probably not a binary.

HD 158614.—If $i = 99°$ (Duncombe & Ashbrook 1952), then $M_1 = 1.00\ M_\odot$ and $M_2 = 0.92\ M_\odot$ (Duquennoy & Mayor 1991). The ΔV is 0.1 mag, and separation is $1''.1$ (Isobe et al. 1992). Both components may contribute variability to the activity record.

HD 178428.—This star is a single-lined spectroscopic binary, with a period near 22 days (Lu 1990; Duquennoy & Mayor 1991). It has a flat activity classification; however, the large intraseasonal scatter about the mean is due to significant shifts in radial velocity arising from orbital motions. The velocity offset (± 14 km s^{-1}) was not compensated in tuning the offset slit and produced short-term fluctuations in S which are not chromospheric in origin.

REFERENCES

Baize, P. 1985, A&AS, 60, 333
Balega, I. I., Balega, Yu. Yu., & Vasyuk, V. A. 1991, Soobschch. Spets. Astrof. Obs., 65, 5
Baliunas, S. L., et al. 1983, ApJ, 275, 752
Baliunas, S. L., et al. 1985, ApJ, 294, 310
Baliunas, S. L., & Jastrow, R. 1990, Nature, 348, 520
Beavers, W. I., & Eitter, J. 1986, ApJS, 62, 147
Beer, J., et al. 1990, Nature, 347, 164
Blazit, A., Bonneau, D., & Foy, R. 1987, A&AS, 71, 57
Brown, T. M., & Morrow, C. A. 1987, ApJ, 314, L21
Bumba, V., & Růžičková-Topolová, B. 1967, Sol. Phys., 1, 216
Buscombe, W. 1977, MK Spectral Classifications: Third General Catalog (Evanston: Northwestern Univ. Press)
———. 1980, MK Spectral Classifications: Fourth General Catalog (Evanston: Northwestern Univ. Press)
———. 1984, MK Spectral Classifications: Sixth General Catalog (Evanston: Northwestern Univ. Press)
Damon, P. E. 1977, in The Solar Output and its Variation, ed. O. R. White (Boulder: Colo. Assoc. Univ. Press), 429
Damon, P. E., & Sonnett, C. P. 1991, in The Sun in Time, ed. C. P. Sonnet, M. S. Giampapa, & M. S. Matthews (Tucson: Arizona Univ. Press), 360
Dobson, A. K., Donahue, R. A., Radick, R. R., & Kadlec, K. L. 1990, in The Sixth Cambridge Workshop on Cool Stars, Stellar Systems and the Sun, ed. G. Wallerstein (ASP Conf. Ser., 9), 132
Donahue, R. A. 1993, Ph.D. thesis, New Mexico State Univ.
Donahue, R. A., & Baliunas, S. L. 1992a, Sol. Phys., 141, 181
———. 1992b, ApJ, 393, L63
Donahue, R. A., Baliunas, S. L., Frazer, J., French, H., & Lanning, H. 1986, in The Fourth Cambridge Workshop on Cool Stars, Stellar Systems and the Sun, ed. M. Zeilik & D. M. Gibson (New York: Springer), 281
Dorren, J. D., & Guinan, E. F. 1994, ApJ, 428, 805
Duncan, D. K., Baliunas, S. L., Noyes, R. W., Vaughan, A. H., Frazer, J., & Lanning, H. 1984, PASP, 96, 707
Duncombe, R. L., & Ashbrook, J. 1952, AJ, 57, 92

Duquennoy, A., & Mayor, M. 1991, A&A, 248, 485
Eddy, J. A. 1976, Science, 192, 1189
———. 1977, in The Solar Output and Its Variation, ed. O. R. White (Boulder: Colo. Univ. Press), 51
Gatewood, G. 1994, PASP, 106, 138
Gilliland, R. L., & Baliunas, S. L. 1987, ApJ, 314, 766
Gough, D. O. 1990, Phil. Trans. R. Soc. Lond., A, 330, 641
Gough, D. O., & Toomre, J. 1991, ARA&A, 29, 627
Hale, G. E. 1908, ApJ, 28, 315
———. 1915, Ten Years Work of a Mountain Observatory (Washington: Carnegie Inst. of Washington)
Hale, G. E., & Fox, P. 1908, The Rotation Period of the Sun as Determined from the Motion of the Calcium Flocculi (Carnegie Inst. of Washington Publ. 93)
Hale, G. E., & Nicholson, S. B. 1925, ApJ, 62, 270
Hardorp, J. 1980, A&A, 91, 221
Hartmann, L., Bopp, B. W., Dussault, M., Noah, P. V., & Klimke, A. 1981, ApJ, 249, 662
Heintz, W. D. 1993, AJ, 105, 1188
Hoffleit, D. 1964, Catalogue of Bright Stars (3d rev. ed.; New Haven: Yale Univ. Obs.)
Hoffleit, D., & Jaschek, C. 1982, The Bright Star Catalogue (4th rev. ed.; New Haven: Yale Univ. Obs.)
Hoffleit, D., Saladyga, M., & Wlasuk, P. 1983, A Supplement to the Bright Star Catalogue (New Haven: Yale Univ. Obs.)
Hoffleit, D., & Warren, W. 1991, The Bright Star Catalogue (5th ed.) in Astronomical Data Center CD ROM, Selected Astronomical Catalogs, 1, ed. L. E. Brotzman & S. E. Gessmer
Horne, J. H., & Baliunas, S. L. 1986, ApJ, 302, 757
Hoyle, F., & Wilson, O. C. 1958, ApJ, 128, 604
Irwin, A. W., Yang, S., & Walker, G. A. H. 1992, PASP, 104, 101
Isobe, S., Noguchi, M., Ohtsubo, J., Baba, N., Miura, N., Tanaka, T., & Ni-ino, M. 1992, Publ. Natl. Astron. Obs. Japan, 2, 459
Keenan, P. C. 1991, PASP, 103, 642
Keil, S. L. 1992, private communication
Keil, S. L., & Worden, S. P. 1984, ApJ, 276, 766
Kovács, G. 1981, Ap&SS, 78, 175
Kraft, R. P. 1967, ApJ, 150, 551
Leighton, R. B. 1959, ApJ, 130, 366
Lippincott, S. L., & Worth, M. D. 1978, PASP, 90, 330
Lu, W.-X. 1990, Chinese Astron., 14, 282
Maunder, E. W. 1890, MNRAS, 50, 251
———. 1894, Knowledge, 17, 173
McAlister, H. A., Hartkopf, W. I., & Franz, O. G. 1990, AJ, 99, 965
Middlekoop, F. 1982, A&A, 107, 31
Morbey, C. L., & Griffin, R. F. 1987, ApJ, 317, 343
Mullen, D. J., & Cheung, Q. Q. 1993, ApJ, 412, 312
Noyes, R. W., Hartmann, L., Baliunas, S. L., Duncan, D. K., & Vaughan, A. H. 1984, ApJ, 279, 763
Parker, E. N. 1955, ApJ, 122, 293
Parker, E. N. 1965, Space Sci. Rev., 4, 666
Rosner, R., Golub, L., & Vaiana, G. S. 1985, ARA&A, 23, 413
Rosner, R., & Weiss, N. O. 1992, in Fourth Solar Cycle Workshop, ed. K. L. Harvey (ASP Conf. Ser., 27), 511
Rutten, R. G. M. 1984, A&A, 130, 353
Saar, S. H. 1994, private communication
Scargle, J. D. 1982, ApJ, 263, 875
Schatzman, E. 1962, Ann. d'Astrophys., 25, 18
Schrijver, C. J. 1993, A&A, 269, 446
Schrijver, C. J., Coté, J., Zwaan, C., & Saar, S. H. 1989, ApJ, 337, 964
Schrijver, C. J., & Rutten, R. G. M. 1987, A&A, 177, 143
Schwabe, H. 1843, Astron. Nach. 20, No. 205
Schwarzschild, K., & Eberhard, G. 1913, ApJ, 38, 292
Sheeley, N. R., Jr. 1967, ApJ, 147, 1106
Silbernagel, E. 1929, Astr. Nach., 234, 441
Skumanich, A. 1972, ApJ, 171, 565
Skumanich, A., Smythe, C., & Frazier, E. N. 1975, ApJ, 200, 747
Slettebak, A. 1963, ApJ, 138, 118
Smith, G., Lambert, D. L., & Ruck, M. J. 1992, A&A, 263, 249
Soderblom, D. R., & Mayor, M. 1993, AJ, 105, 226
Soon, W. H., Zhang, Q., Baliunas, S. L., & Kurucz, R. L. 1993, ApJ, 416, 787
Spörer, F. W. G. 1887, Vierteljahrsschr. Astron. Ges. (Leipzig), 22, 323
———. 1889, Bull. Astron., 6, 60
Stauffer, J. R. 1991, in Angular Momentum Evolution of Young Stars, ed. S. Catalano & J. R. Stauffer (Dordrecht: Kluwer), 117
Steenbeck, M., Krause, F., & Rädler, K.-H. 1966, Z. Nat. 21a, 369
Stephenson, C. B. 1960, AJ, 65, 60
Tokovinin, A. A., & Ismailov, R. M. 1988, A&AS, 72, 563
van den Bos, W. H. 1937, Union Obs. of S. Africa Circ., 4, 342
Vaughan, A. H., Baliunas, S. L., Middlekoop, F., Hartmann, L. W., Mihalas, D., Noyes, R. W., & Preston, G. W. 1981, ApJ, 250, 276
Vaughan, A. H., & Preston, G. W. 1980, PASP, 92, 385
Vaughan, A. H., Preston, G. W., & Wilson, O. C. 1978, PASP, 90, 267
Waldmeier, M. 1961, The Sunspot Activity in the Years 1610–1960 (Zurich: Schulthess)
White, O. R., & Livingston, W. C. 1978, ApJ, 226, 679
———. 1981, ApJ, 249, 798
White, O. R., Skumanich, A., Lean, J., Livingston, W. C., & Keil, S. L. 1992, PASP, 104, 1139
Wilson, O. C. 1963, ApJ, 138, 832
———. 1966, ApJ, 144, 695
———. 1968, ApJ, 153, 221
———. 1976, ApJ, 205, 823
———. 1978, ApJ, 226, 379
———. 1984, private communication
Wilson, O. C., & Bappu, M. K. V. 1957, ApJ, 125, 661
Wilson, O. C., & Skumanich, A. 1964, ApJ, 140, 1401
Wolf, R. 1856, Astron. Mitt. Zurich, No. 14
Wolff, S. C., Boesgaard, A. M., & Simon, T. 1986, ApJ, 310, 360